Inorganica Chimica Acta 443 (2016) 64–68

Contents lists available at ScienceDirect

Inorganica Chimica Acta

journal homepage: www.elsevier.com/locate/ica

Guest water-controlled reversible crystalline-to-amorphous transition and concomitant fluorescence shift in a polar open coordination polymer

Lingyun Xin [a], Guangzhen Liu [a,*], Lufang Ma [a], Guilian Li [a], Liya Wang [a,b,*]

[a] College of Chemistry and Chemical Engineering, Luoyang Normal University, Luoyang, Henan 471022, PR China
[b] College of Chemistry and Pharmacy Engineering, Nanyang Normal University, Nanyang, Henan 473061, PR China

ARTICLE INFO

Article history:
Received 29 October 2015
Received in revised form 18 December 2015
Accepted 19 December 2015
Available online 30 December 2015

Keywords:
Coordination polymer
Crystal-to-amorphous transformation
Fluorescence shift

ABSTRACT

This work presents a polar porous coordination polymer with new topological prototype, named {[Zn(ndca)(bpp)]·$(H_2O)_5$}$_n$ (H_2ndca = 5-norbornene-2,3-dicarboxylic acid and bpp = 1,3-bis(4-pyridyl) propane). Each the borehole-shaped linear channel is encapsulated with one spiral water tape built by alternate array of the quadrangular and hexagon water clusters. The crystals display a reversible crystal-to-amorphous transformation through subtly manipulating over the evacuation and uptake of the guest water tapes confined in the channels upon performing the dehydrated-rehydrated process and I_2-exchanged experiment. The results show that the polar crystalline structure is stabilized by the well-orientated H-bonds between the host framework and guest water tape, which are also responsible for the prefect host-guest chiral matching. The most distinguished feature for this material is attribuated to the reversible crystalline-to-amorphous phase transition that is accompanied with a significant fluorescence shift by 31 nm, implying its great potential in fluorescence sensing of the environment humidity.

1. Introduction

Microporous coordination polymers (CPs) have received much attention due to their great potentials in storage and separation [1–4], heterogeneous catalysis [5–8], sensor technology [9–12], and drug delivery [13–16]. Among them, the flexible framework with dynamic structure feature are of great interest due to their enhanced capacity of the solid-state structure transformations through guest evacuation/uptake, ligand/metal exchange, framework shrinkage/ swelling [17–19], and structure rearrangement/-transition upon exposure to various external stimulis such as light, electricity, magnetism, thermal, and stress [20,21]. Noted that the solid-state structure transformations are usually accompanied with drastically adjustable function performance that is estimated to make the flexible CPs ideal as molecular devices such as switches and sensors, magnetism, and electricity [22,23]. And what is more, some flexible CPs have the ability to adapt their pore opening to various guest molecules, even displaying a gate-open behavior [24,25]. Of the solid-state structure transformations, the stimuli-induced crystalline-to-crystalline transformation (CCT) is frequently observed in a wide variety of CPs [26,27].12 The crystalline-to-amorphous transformation (CAT) and amorphous-to-crystalline transformation (ACT) are relatively less common [28,29] as both processes are related to the extremely severe structure transitions between the order and disorder that is infeasible in the ordinary sense, although they are highly desirable for CPs with the improved selectivity and sensitivity of function responses.

Herein, we present a polar 2D CP with new framework topology, {[Zn(ndca)(bpp)]·$5H_2O$}n (**1**·$5H_2O$), hydrothermally prepared by a mixed-ligand strategy with the combination of a rigid dicarboxylic acid and flexible dipyridyl-type ligand (H_2ndca = 5-norbornene-2,3-dicarboxylic acid and bpp = 1,3-bis(4-pyridyl) propane) (Scheme 1). The subtle implementation of the evacuation and implantation of spiral water tape confined in the linear channel induces the reversible crystal-to-amorphous phase transition by exerting very gentle external stimuli, e.g. heating in air above 60 °C or I_2-exchange at room temperature, accompanying with significant fluorescence shift by 31 nm.

2. Experimental

2.1. Materials and physical measurements

All reagents and solvents for synthesis and analysis were commercially available and used as received. Elemental analyses (CHN)

---

* Corresponding authors at: Tel.: +86 0379 65515113 (G. Liu). College of Chemistry and Chemical Engineering, Luoyang Normal University, Luoyang, Henan 471022, PR China. Tel.: +86 0379 65523593 (L. Wang).

E-mail addresses: gzliuly@126.com (G. Liu), wlya@lynu.edu.cn (L. Wang).

http://dx.doi.org/10.1016/j.ica.2015.12.022
0020-1693/© 2015 Elsevier B.V. All rights reserved.

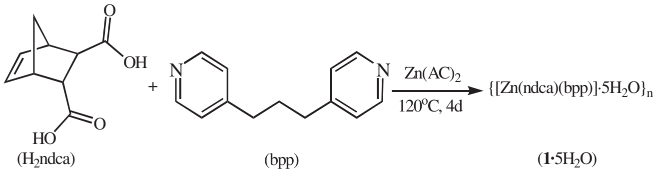

Scheme 1. The synthesis route of **1**·5H_2O.

were performed on a Flash EA 2000 elemental analyzer. Fourier transform infrared spectroscopies (FT-IR) were recorded with a Nicolet 6700 spectrophotometer over a range 4000–600 cm^{-1}. Luminescence spectra of the solid samples were performed on a Hitachi F-4500 fluorescence spectrophotometer at room temperature. Thermogravimetric analysis (TGA) experiments were carried out on a SII EXStar6000 TG/DTA6300 analyzer under a dry nitrogen atmosphere with a heating rate of 10 °C min^{-1}. The powder X-ray diffraction patterns (PXRDs) were recorded with a Bruker AXS D8 Advance diffractometer using monochromated Cu Kα radiation (λ = 1.5418 Å).

2.2. Synthesis of {[Zn(ndca)(bpp)]·5H_2O}$_n$ (**1**·5H_2O)

$Zn(OAc)_2 \cdot 2H_2O$ (0.022 g, 0.10 mmol), 5-norbornene-2,3-dicarboxylic acid (H_2ndca) (0.018 g, 0.10 mmol), and 1,3-bis(4-pyridyl) propane (bpp) (0.020 g, 0.10 mmol) were dispersed in mixed solvent H_2O/EtOH (v:v = 3/1; 6 mL), followed by the addition of NaOH (0.002 g, 0.05 mmol). The mixture was transferred to in a 23 mL Teflon liner stainless steel reactor and heated at 120 °C for 4 days under static conditions, and then cooled to room temperature. Colorless block crystals were separated and washed with deionized water and allowed to dry in air (0.031 g, yield 58% based on ZnO). *Anal.* Calc. for $C_{22}H_{32}N_2O_9Zn$ (**1**·5H_2O): C, 49.50; H, 6.04; N, 5.25. Found: C, 50.11; H, 5.89; N, 5.62%. Selected IR (KBr, cm^{-1}): 3370 (m), 2962(w), 1606(s), 1560(m), 1434(s), 1402(s), 1341(m), 1282 (s), 1252(w), 1232(m), 1214(m), 1082(m), 1069(m), 1029(m), 913 (w), 884(w), 841(m), 818(m), 802(s), 763(m), 736(m), 713(m).

2.3. X-ray crystallography

The crystallographic data collections were carried out a Bruker *SMART APEX II* CCD diffractometer equipped with graphite-monochromated Mo Kα radiation (λ = 0.71073 Å) by using φ/ω scan technique at room temperature. The structures were solved by direct methods followed by successive difference Fourier syntheses, and a full-matrix least-squares refinement on F^2 was carried out using the SHELX-97 program [30,31] package with anisotropic thermal parameters for all non-hydrogen atoms. All non-hydrogen atoms were easily found from the Fourier difference maps, whereas the H atoms were placed in calculated positions and refined isotropically with a riding model. The details of the structure solutions and final refinements for **1**·5H_2O are summarized in Table 1. Selected bond distances/angles and hydrogen bonds are listed in Tables S1 and S2.

3. Result and discussions

3.1. Structural description of {[Zn(ndca)(bpp)]·5H_2O}$_n$ (**1**·5H_2O)

The structure displays a chiral metal-organic coordination layer with the borehole-shaped linear channel encapsulated with a spiral water tape. The asymmetric unit consists of one unique Zn(II) ion, one ndca dianion, one bpp molecule, and five lattice waters (Fig. S1, ESI†). The first coordination sphere of Zn(II) cation is defined by two bpp N atoms (Zn(1)–N(1) = 2.062(6) and Zn(1)–N (2) = 2.081(2) Å) (Table S1, ESI†) and two ndca carboxylate O atoms (Zn(1)–O(1) = 1.989(2) Å and Zn(1)–O(3) = 2.035(2) Å) to form a distorted tetrahedral geometry. Each ditopic ndca carboxylate bridges two Zn(II) ions in a bis(monodentate) coordination mode to form a right-hand 2^1 Zn-carboxylate helical chain propagating along the b direction (Fig. S2, ESI†). All homochiral helixes are parallelly positioned and cross-linked by interchain bpp coligands to develop a chiral layer with the borehole-shaped linear channels paralleling to both the helix and the layer (Fig. 1a and b). Topology analysis gives a previously unknown 4-connected net with point (Schläfli) symbol of {$4^2.6^3.8$}, designated as LYU-5 (Fig. S3, ESI†). Noted that the chiral layers are arranged along the c direction in a -AAA- stacking fashion and are cohered by the weak van der Waals force to form a polar 3D supermolecular network (Fig. S4, ESI†).

The linear channel with the 3.17 × 3.27 Å aperture (excluding the van der Waal radii of the surface carbon atoms) (Fig. S5, ESI†) is encapsulated with one spiral water tape related by a 2_1 screw axis, which is assembled by the alternate array of quadrangle and hexagon water clusters decorated by two lateral water arms (O9) (Fig. 1c). Besides the specific intra-tape H-bonds with $O_w \cdots O_w$ distances of 2.758(4)–3.265(11) Å, each spiral water tape is further supported and stabilized by the host-guest H-bonds between the carboxylate oxygens and the lattice waters with $O_{carboxylate} \cdots O_w$ distances of 2.810(4)–2.897(3) Å (Table S2, ESI†). It has been demonstrated that the water clusters play a crucial role in contributing to the stability and function of biological assemblies and manipulating the proton conductivity [32] and even the ferroelectricity [33] of CPs.

Table 1
Crystal and structure refinement data for **1**·5H_2O.

	1·5H_2O		**1**·5H_2O
Empirical formula	$C_{22}H_{32}N_2O_9Zn$	Z	4
Formula weight	533.87	D_{calc} (g cm^{-3})	1.361
T (K)	296(2)	μ (mm^{-1})	0.992
Crystal system	Monoclinic	F(000)	1120
Space group	C2	θ (°)	2.36–25.50
a (Å)	21.213(2)	Reflections collected	9977
b (Å)	10.4270(12)	Independent reflections	4640
c (Å)	15.455(3)	R_{int}	0.0188
α (°)	90	Data/restraints/parameters	4640/1/308
β (°)	130.3370(10)	Goodness-of-fit (GOF)	1.022
γ (°)	90	Final R indices [$I > 2\sigma(I)$]	R_1 = 0.0310, wR_2 = 0.0849
V (Å^3)	2605.8(7)	R indices (all data)	R_1 = 0.0335, wR_2 = 0.0865
Flack parameter	−0.003(11)	Largest difference peak/hole (e A^{-3})	0.682/−0.194